Temperature dependent photoluminescence of nanocrystalline γ-CuCl hybrid films

M.M. Alam [a,*], F. Olabanji Lucas [a], D. Danieluk [b], A.L. Bradley [b], S. Daniels [a], P.J. McNally [a]

[a] Nanomaterials Processing Laboratory, School of Electronic Engineering, Dublin City University, Dublin 9, Ireland
[b] Semiconductor Photonics Group, Physics Department, Trinity College Dublin, Dublin 2, Ireland

A B S T R A C T

Organic–inorganic hybrid films combine the basic properties of organic and inorganic materials and offer special advantages that enhance optical, thermal and mechanical properties. We have studied the temperature dependent photoluminescence (PL) of nanocrystalline γ-CuCl hybrid films from 15 K to room temperature in order to investigate the electronic transitions of the hybrid films. The I_1 impurity bound exciton peak is the most intense emission peak at 15 K but the peak intensity decreases rapidly with increasing temperature due to the low binding energy of this exciton bound to an impurity center and above 80 K all three excitonic and biexcitonic peaks, except the Z_3 free exciton emission peak disappeared. The biexciton emission peak intensity follows a quadratic dependency on power in the excitation power range <10 kWcm^{-2}. The integrated Z_3 excitonic PL intensity is almost independent of the temperature below 80 K, while above 100 K the PL emission intensity decreases rapidly. Thermal quenching of the Z_3 free exciton PL emission in hybrid films has been observed. The full width at half maximum (FWHM) of the free exciton peak was investigated as a function of temperature and was explained by a theoretical model which considers the scattering of excitons with acoustic phonons and longitudinal optical phonons. The FWHM of the Z_3 free exciton emission peak increases with increasing temperature, and a value of ~76 meV was deduced for the FWHM at room temperature, which is comparatively better than ZnO (106 meV) and GaN (100 meV) nanostructures. The Z_3 free exciton energy of the hybrid films exhibits a blue shift of 3 meV at 15 K compared to the bulk CuCl samples which may be due to a dead layer effect near the CuCl nanocrystal surface. The exciton energy also presents a blue shift of ~41 meV with increasing temperature from 15 K to room temperature. The results obtained for the γ-CuCl hybrid films are comparable to those of vacuum evaporated and sputtered CuCl films reported in the literature.

1. Introduction

CuCl luminescence has been investigated extensively for many years, owing to its interesting structural, optical and electrical properties [1–6]. It is an ionic I-VII compound wide direct band gap semiconductor material with the zinc blende structure. It has attracted renewed interest due to several characteristics such as possessing free exciton binding energies of approximately 190 meV, which are much larger than for III-nitride, III-V and II-VI semiconductors [1]. Due to this large excitonic binding energy CuCl hybrid films have intense Z_3 free exciton PL emission in the UV spectral region at room temperature. Its biexciton binding energy is about 32 meV [7] and biexciton lasing action from CuCl quantum dots embedded in a NaCl matrix has also been reported [8]. At low temperature CuCl exhibits a strongly negative linear expansion coefficient and elastic shear constants that decrease with increasing hydrostatic pressure which are related to an anharmonic lattice potential [3]. In general, the photoluminescence emission intensity of a semiconductor and ionic crystal decreases monotonically with increasing temperature. This phenomenon is called “thermal quenching” of photoluminescence [9]. In other words the “thermal quenching" phenomenon can be defined as the increase of the non-radiative recombination probability of electrons and holes with increasing temperature. The thermal quenching phenomenon and its theoretical analysis have been extensively studied to describe the temperature dependent photoluminescence intensity of various materials [10–14].

Organic–inorganic hybrid materials are receiving growing attention for building and testing electronic and optoelectronic devices [15–17]. Temperature dependent PL spectroscopic measurements provide a useful insight into the electronic transitions of materials. Thus, in this paper, we present the results of the temperature dependent photoluminescence of γ-CuCl nanocrystalline hybrid films deposited via spin coating techniques in order to determine the thermal quenching behavior and its electronic transitions.

2. Experimental details

The γ-CuCl nanocrystalline hybrid films with typical layer thicknesses of ~200 nm were deposited on glass or flexible substrates by the spin coating method using a Laurell WS-400A-6PP/LITE spin coater in a class 100 clean room to avoid contamination. The coating was performed at room temperature. The nanocrystals were synthesized by a complexation–reduction–precipitation mechanism reaction of $CuCl_2 \cdot 2H_2O$, alpha D-glucose and de-ionized water with an organic polysilsesquioxane (PSSQ) based solution as the host matrix material. The films were subsequently heated at 120 °C for 18 hours *in vacuo*. After heating the films, X-ray diffraction (XRD) confirmed the preferential growth of CuCl nanocrystals whose average size is ≈35 nm in the ⟨111⟩ orientation. The details of the solution processes, synthesis and film deposition were described previously [2]. The luminescence properties were studied using temperature dependent photoluminescence spectroscopy in the range between 15 K to room temperature, by employing a UV Ar^+ Innova laser with a second harmonic generation barium borate crystal producing a 355 nm photoexcitation. The PL spectra were collected on a Jobin Yvon-Horiba Triax 190 spectrometer with a spectral resolution of 0.3 nm, coupled with a liquid nitrogen-cooled CCD detector. The samples were kept under vacuum during the PL measurement, to prevent the oxidation of CuCl nanocrystal hybrid films.

3. Results and discussion

3.1. Excitonic transitions in γ-CuCl hybrid film

The photoluminescence spectra acquired at different temperatures in the range between 15 and 300 K are shown in Fig. 1. Figs. 2 and 3 show the contributions of different recombination centers connected with emission peaks at 15 K and 300 K, respectively. The CuCl photoluminescence peaks were fitted with Lorentzian line shapes to find the FWHM. There are four peaks evident in the spectra measured from 15 to 60 K. At 15 K, the peak centered at 3.213 eV (≈385.9 nm) is the Z_3 free exciton peak (Figs. 1 and 2) whereas the room temperature Z_3 free exciton PL emission is at 3.254 eV (≈381 nm) which is shown in Fig. 3. The exciton emission energy increases from 3.213 eV at 15 K to 3.254 eV at room temperature. Moving to longer wavelengths of the emission spectra of Figs. 1 and 2, one can observe a peak occurring at 3.191 eV (≈388.6 nm). This peak is attributed to emission from an exciton bound to an impurity, which has been called the I_1 impurity bound exciton and the impurity or defect involved in this process has been previously identified as a neutral acceptor, possibly a Cu vacancy [2,18]. The peak at 3.170 eV (≈391.2 nm) is identified as a free biexciton M [19]. The low intensity peak at 3.141 eV (≈394.7 nm) conventionally labeled

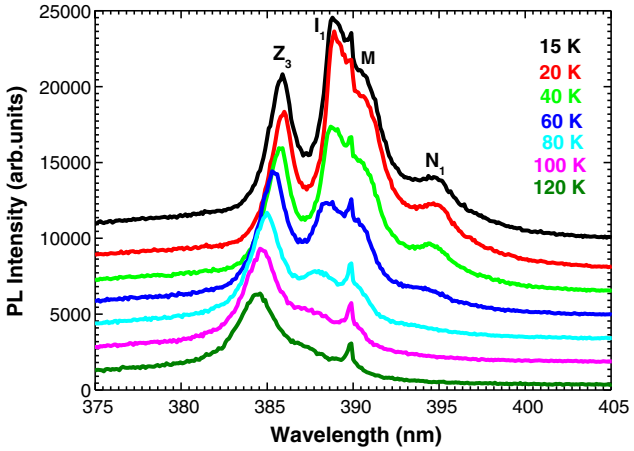

Fig. 1. Photoluminescence spectra of CuCl hybrid film at different temperatures.

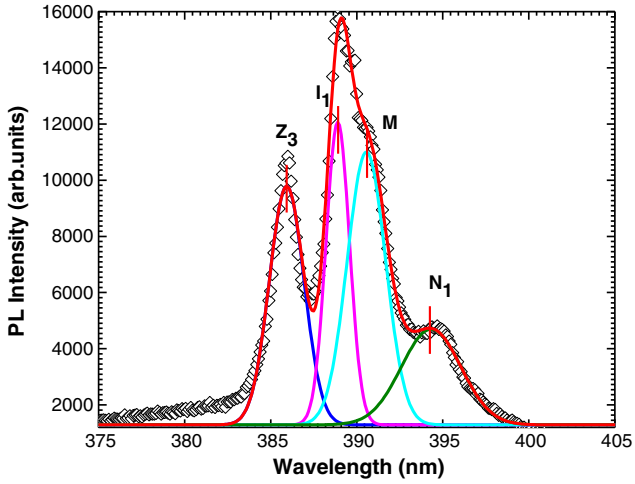

Fig. 2. Fitted photoluminescence spectra of CuCl hybrid films with fit (solid curve) based on Lorentzian line shapes at 15 K.

N_1 is evident, and likely originates from a biexciton bound to an impurity. Similar to the I_1 bound exciton, the most probable candidate for this impurity is a neutral acceptor [1]. The intensities of the impurity bound exciton (I_1) and the impurity bound biexciton (N_1) peaks decrease more rapidly in comparison with the free exciton (Z_3) peak as the temperature increases. In the temperature range from 60 K to room temperature, the spectra were dominated by the Z_3 free exciton peak. The dominance and the stability of the Z_3 exciton peak are due to the large binding energy of the order 190 meV. The bound exciton and biexciton both disappear simultaneously at 100 K. Fig. 4 shows the variation the of excitonic (Z_3) and biexcitonic (M) and bound biexciton (i.e. N_1) emission intensities with excitation power analyzed on a double logarithmic scale for the CuCl hybrid film at 15 K. Excitation power dependent PL measurements can be used to confirm the excitonic or biexcitonic nature of the emission. For low power excitation conditions, the excitonic and bound biexcitonic PL emission displays a linear dependence on excitation power, whereas free biexcitonic PL emission typically displays a quadratic dependence on excitation power [20,21]. The biexciton emission intensities for the CuCl hybrid film clearly show an approximately quadratic dependency on excitation power for lower excitation power densities of <10 kWcm^{-2}. The free exciton and bound biexcitons show an approximately linear dependence on power, similar to results reported by other researchers for CuCl nanocrystals embedded in NaCl matrices and InGaAs/GaAs quantum

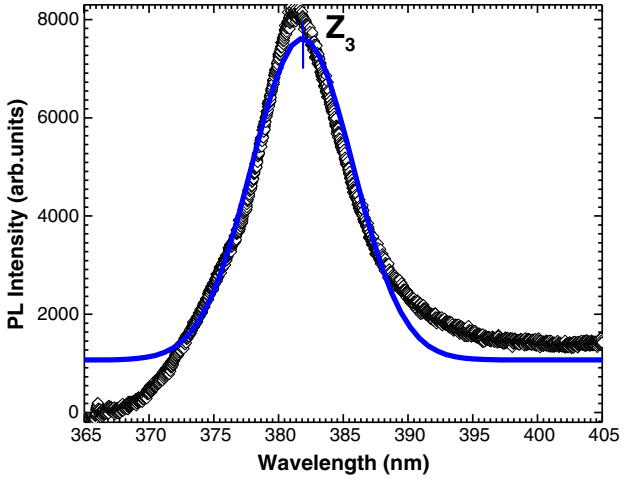

Fig. 3. Photoluminescence spectra of CuCl hybrid films with fit (solid curve) based on Lorentzian line shapes at 300 K.

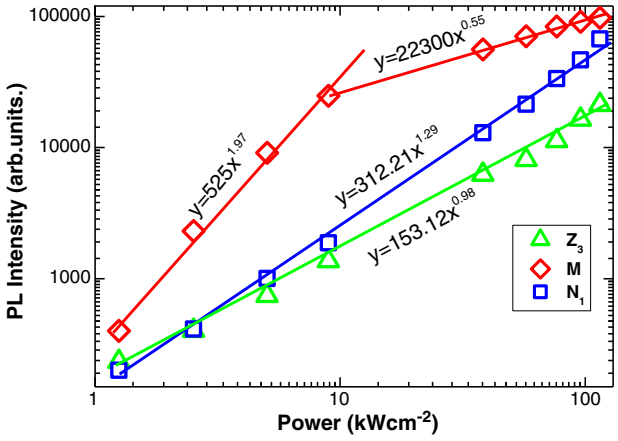

Fig. 4. Excitonic, biexcitonic and bound biexciton emission line intensity vs. excitation power analysis in double logarithmic scale.

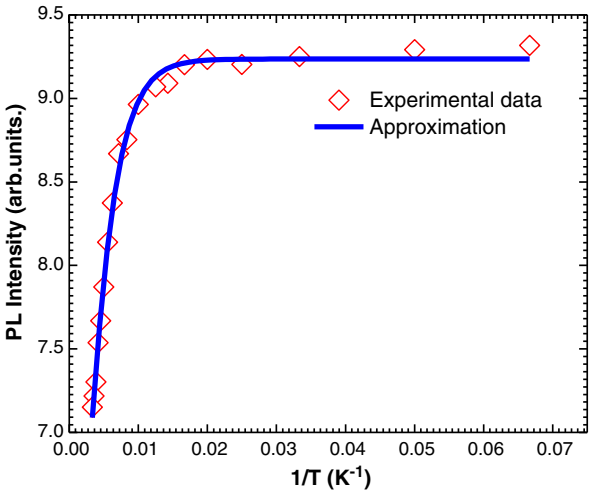

Fig. 5. A plot of the integrated Z_3 excitonic PL intensity vs. inverse temperature. Fitting with a two-step thermal quenching process is shown with a solid line for CuCl hybrid film.

dash structures [8,21,22]. For the higher excitation regimes the biexciton emission intensities appear to have a linear dependence on power. Phillips et al. suggested that this reversion to an approximately linear dependence was due to shorter recombination times of biexcitons in such direct-band gap materials [23]. The binding energy of the bound exciton (E^b_{bX}), the free biexciton (E^b_{XX}) and the bound biexciton (E^b_{bXX}) of the nanocrystalline CuCl hybrid film can be calculated by using the energy calculation scheme based on Eqs. (1–3) [4,34]:

$$E^b_{bX} = E_X - E_{bX} \tag{1}$$

$$E^b_{XX} = E_X - E_{XX} \tag{2}$$

$$E^b_{bXX} = 2E_X - E_{bXX} - E_{bX} - E^b_{XX} \tag{3}$$

where E_X (3.213 eV), E_{XX} (3.170 eV), E_{bX} (3.191 eV) and E_{bXX} (3.141 eV) are the free exciton, biexciton, bound exciton and bound biexciton energies, respectively, taken from the PL spectrum at 15 K as shown in Figs. 1 and 2. The calculated binding energy of the bound exciton is about 22 ± 2 meV and is in excellent agreement with previously reported values for vacuum deposited CuCl thin film on silicon substrates [5] and bulk CuCl [24]. The free biexciton binding energy is 43 ± 2 meV, which is approximately 11 meV higher than reported for bulk CuCl and almost the same as for CuCl quantum dots embedded in NaCl matrices [24]. Though the mechanism for the increase in the biexciton binding energy is not entirely clear at present [25], it is known that the biexciton binding energy significantly increases with decreasing crystal size as reported by Masumoto et al. [24]. The calculated bound biexciton binding energy is 51 ± 2 meV; this value is ~7 meV less than for CuCl films deposited on silicon substrates [5]. This is considerably larger than the biexciton binding energies of II-VI semiconductors such as ZnSe, CdS, and ZnO (BM_3 and BM_7 band) which are approximately 3.5, 6.3 and 15 meV, respectively [26]. The high quality biexciton (two confined electron–hole pairs) can be used as a quantum bit pair for quantum processing, as was shown conceptually in Edamatsu et al. [27].

3.2. Thermal quenching of PL intensity

A plot of the natural logarithm of the integrated Z_3 excitonic PL intensity as a function of inverse temperature is shown in Fig. 5. One can observe clearly that the PL emission intensity is almost independent of temperature below 80 K, and above 100 K the PL emission intensity decreases rapidly. Therefore, the thermal quenching of the Z_3 PL emission can be described by means of a two-step process, and the experimental data are fitted by Eq. (4) below [28,29]:

$$I = I_0 / \left(1 + \mathrm{A}\exp\left(\frac{-\mathrm{E}_1}{kT}\right) + \mathrm{B}\exp\left(\frac{-\mathrm{E}_2}{kT}\right)\right) \tag{4}$$

where E_1 and E_2 are the thermal activation energies and A and B are constants related to the lifetime of the excited state and the effective scattering time from the excited state to the non-radiative center. These thermal activation energies were calculated to be $E_1 \approx 23$ meV and $E_2 \approx 140$ meV, respectively. The higher thermal activation energy (≈140 meV) connected with the thermal dissociation of the free excitons should be same as the binding energy of the excitons. This calculated value is lower than the exciton binding energy of 190 meV [1] but in agreement with the reported thermal activation energy for CuCl films on silicon substrates [34], higher than for sputtered CuCl films [6] and lower than the value (150 meV) reported for single crystal CuCl [30,31]. This value indicates that the hybrid films' excitonic properties lie between those of the sputtered and single crystal CuCl films. Since the other activation energy $E_1 \approx 23$ meV lies close to the biexciton binding energy values it is reasonable to associate this thermal activation energy with the biexciton bound impurity [32].

3.3. Exciton line broadening

The full width at half maximum of the Z_3 free exciton PL emission peak increases with temperature due to increased exciton–phonon interactions [33]. The PL emission peak was fitted to a Lorentzian distribution to estimate the full width at half maximum. Fig. 6 shows the variation of the FWHM of the Z_3 free exciton emission peak for a typical CuCl hybrid film. The FWHM experimental data are fitted with the following expression [5]:

$$\Gamma = \Gamma_0 + \gamma_{LA}T + \frac{\gamma_{LO}}{\left(\exp\left(\frac{nh\nu_{LO}}{kT}\right) - 1\right)} \tag{5}$$

where Γ is the line width broadening of free exciton line, n is the number of phonons involved, Γ_0 is the FWHM of the Z_3 free exciton emission peak at 0 K, γ_{LA} and γ_{LO} describe the interaction of excitons with longitudinal acoustic and optical phonons of the lattice, respectively. $h\nu_{LO}$ (26 meV) is the energy of the LO phonon of CuCl [34] and T is the temperature. By fitting the experimental data with Eq. (5) the following parameters were extracted: $\Gamma_0 = 7.25 \pm 0.025$ meV, $\gamma_{LA} \approx 30 \pm 0.2$ μeVK^{-1}, $\gamma_{LO} \approx 945 \pm 2$ meVK^{-1} and $nh\nu_{LO} = 70.15 \pm 3.5$ meV. The value of $nh\nu_{LO}$

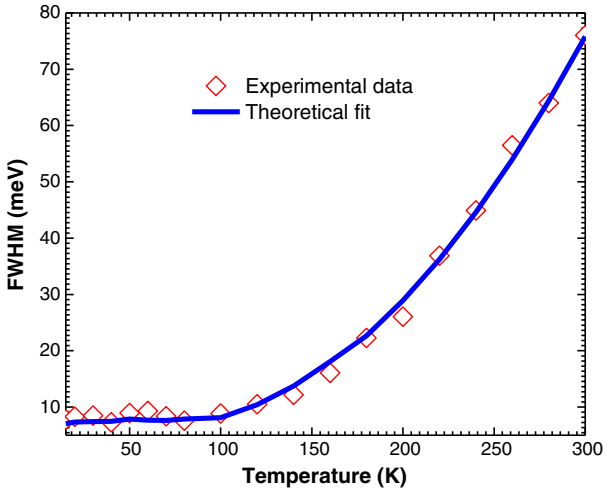

Fig. 6. Temperature dependence of full width at half maximum of the CuCl hybrid film Z_3 free exciton peak; the solid line is the theoretical fit.

is ~70 meV, which suggests that 3 phonons are involved in the exciton–phonon interaction (i.e. $3 \times h\nu_{LO} \approx 78$ meV) [35]. The values of γ_{LA} and γ_{LO} are larger than the values reported for ZnO [55] and GaN [36], and, interestingly, are also higher than for sputtered CuCl films [6]. This suggests that the CuCl hybrid film appears to have a stronger exciton–phonon interaction than these other semiconductors, which is most likely due to the polar nature of CuCl bonding [37] From Fig. 6 it is clear that the increase of the FWHM at temperatures below 120 K is quite linear and very small, while above 120 K to room temperature the FWHM increases exponentially. This indicates that up to 120 K acoustic phonons contribute and above 120 K the LO optical phonons are mostly responsible for the increase of FWHM [36]. The FWHM of the room temperature Z_3 PL emission peak is ~76 meV for the CuCl nanocrystalline hybrid films and is in excellent agreement with earlier reports for sputtered CuCl film (74 meV) [6], and comparatively better than GaN (100 meV) [38] and ZnO (106 meV) [39] nanostructures for UV light emitting materials.

3.4. Exciton energy shifting

The Z_3 transition occurs at an energy of 3.213 eV (≈385.9 nm) at 15 K. This represents a blue shift of approximately 3 meV compared to the Z_3 transition energy in bulk CuCl of 3.210 eV (≈386.3 nm) [40]. In CuCl nanocrystals, the size dependent blue shift of the exciton energy can be expressed by an exciton quantum confinement model described by the following expression [41]:

$$\Delta E = \frac{\hbar^2 \pi^2}{2M(a^*)^2} \tag{6}$$

where ΔE is the blue shift of the exciton energy, M is the Z_3 excitation translation mass ($M = 2.3\ m_0$, where m_0 is the electron rest mass) and $a^* = a - 0.5a_B$, where a is the radius of the CuCl nanocrystals and a_B is the Bohr radius of the exciton (0.7 nm for CuCl) [42]. Using the measured blue shift of $\Delta E \approx 3$ meV, an average CuCl nanocrystal radius of 7.73 nm is obtained. To observe the strong or weak quantum confinement effect the radius of the particle should be close to the Bohr radius ($R/a_B \leq 2$ for strong and $R/a_B \leq 4$ for weak confinement). However in our measurements the radius of CuCl is more than 11 times greater than the CuCl Bohr radius. Thus it is unlikely that the blue shift is due to the phenomenon of exciton quantum confinement.

Another cause could be pressure and polarization effects induced by the PSSQ matrix. A hydrostatic pressure induced exciton energy shift in bulk CuCl (7.65 meV/GPa) [43], for CuCl microcrystals embedded in alkali-chloride matrices (8.22 meV/GPa) [44] and for nanocrystals in a LiCl matrix (4.1 meV/GPa) [45] were reported previously. The hydrostatic pressure in nanocrystalline CuCl hybrid films is, however, very small, so the energy shift associated with this effect is not considerable. Brus reported that there is a polarization effect on the exciton energy for microcrystals surrounded by a dielectric matrix. The change of exciton energy ΔE is assumed to be mainly associated with the exciton internal motion and is expressed by [46]:

$$\Delta E = \frac{6(\varepsilon_2 - \varepsilon_1)}{\varepsilon_2 + 2\varepsilon_1}\left(\frac{a_B}{R}\right)^3 Ryd^* \tag{7}$$

where ε_1 and ε_2 are the dielectric constants of the PSSQ matrix and CuCl, respectively, $Ryd^* = 213$ meV for CuCl [47], and R is calculated to be about ~3.39 nm, which is smaller than the nanocrystal radii obtained via XRD analysis, but is at least of the same order.

Another cause of this blue shift may be the presence of micro-strain in the CuCl nanocrystals embedded in the PSSQ matrices. Generally, the crystal symmetry can be altered by strain in the film. A variation in the crystal symmetry is reflected in the electronic band structure and shifts the energy levels. Uniaxial stress on semiconductors produces a change in the lattice constant and symmetry of the crystal, and as a consequence, these cause important changes in the electronic properties. A Z_3 free exciton energy increase due to the uniaxial stress was reported by T. Koda et al. [48]. The film strain along the lattice constant axis, a, can be measured using the following expression [49]:

$$\varepsilon = \left(\frac{a_s - a_o}{a_o}\right) \times 100\% \tag{8}$$

where $a_o = 5.4160$ Å is the lattice constant of unstrained CuCl [50] and $a_s = 5.4337$ Å is the lattice parameter of the CuCl hybrid films calculated from the XRD data. Computing the strain using the above relationship we found that the hybrid films are under tensile strain of approximately +0.32%. According to the work of Kim et al. [51] and Blacha et al. [44] the tensile strain induced shift in the observed exciton energy should be ≈−1.31 meV, i.e. a red shift when in fact the observed exciton energy reported herein is blue shifted. Thus it is unlikely that strain the major source of the observed blue shift of 3 meV. For nanocrystals with $R > a_B$, the electron and hole motion around their center of mass prevents the center of mass from reaching the nanocrystal surface, thus forming a layer which is called a "dead layer" near the nanocrystal surface. In other words the near surface regions cannot be reached by the center of mass of the exciton due to the finite size of the quasiparticle. Taking the exciton dead layer into account, the exciton energy shift can be expressed as [52]:

$$\Delta E = \frac{\hbar^2 \pi^2}{2M(R - \eta a_B)^2} \tag{9}$$

where η is a constant whose numerical value is a function of m_h^*/m_e^*; for $m_h = 4.2\ m_0$ and $m_e = 0.43\ m_0$ [53] then $\eta = 9.77$. The nanocrystal radius was calculated using above values and was found to be ~14.23 nm, whose value is close to the value of nanocrystals radius (~17.5 nm) obtained from XRD analysis.

From the above investigation, the radius of the CuCl crystal is much larger than its Bohr radius for the quantum confinement effect to play a major role; the hydrostatic pressure is also too small to account for the exciton energy shifts. The CuCl crystal radius obtained by considering the polarization effect on the exciton energy is also ~5 times smaller than the value obtained by XRD analysis and this is not considerably significant. Strain effects are also not considered likely. The radius of the CuCl crystals calculated by considering the operation of a dead layer effect (~14.23 nm) is very close to the value obtained by XRD analysis (~17.5 nm) therefore it is likely that the observed blue shift in the nanocrystalline CuCl hybrid films can be attributed to a dead layer effect near the CuCl nanocrystal surface.

3.5. Exciton line shift with temperature

The variation of the CuCl hybrid film Z_3 free exciton emission peak position as a function of temperature is shown in Fig. 7. This reveals that the effective exciton binding energy increases from 3.213 eV at 15 K to 3.254 eV at room temperature. This blue shift as a function of temperature is in contrast to other semiconductors, i.e. the variation of band gap energy of CuCl in hybrid films does not follow the Varshni or Einstein models [5,54,55]. The Z_3 exciton binding energy shift as a function of temperature for the CuCl hybrid film is similar to those previously reported for vacuum evaporated and sputtered CuCl thin film [5,6]. The binding energy increase with increasing temperature can be explained on the basis of the model of Garro et al. who postulated that the Cu ions vibrating principally at low frequencies lead to an increase in the binding energy, whereas the Cl ions, vibrating at high frequencies, lead to a reduced exciton binding energy [56]. When these two competing processes are taken together, the exciton binding energy tends to increase at low temperature (<70 K) and will continue to increase, but above 70 K the band gap increase rate is significantly reduced.

To explain the energy shift as a function of temperature the experimental data was fitted by using the two oscillator model proposed by Göbel et al. [3]. They describe the mass (Cu and Cl) and temperature dependence of the exciton binding energy in the following expression [3]:

$$E(T,M) = E_0 + \frac{A_{Cu}}{\nu_{Cu}M_{Cu}}\left(\frac{1}{\exp(h\nu_{Cu}/k_BT)-1}+\frac{1}{2}\right) + \frac{A_{Cl}}{\nu_{Cl}M_{Cl}}\left(\frac{1}{\exp(h\nu_{Cl}/k_BT)-1}+\frac{1}{2}\right) \quad (10)$$

where ν_{Cl} and ν_{Cu} are the phonon frequencies of Cl and Cu (6 THz and 1 THz, respectively), E_0 is the unrenormalized exciton binding energy, and A_{Cu} and A_{Cl} are the electron–phonon interaction parameters for copper and chlorine, respectively, which can be determined from the fitting of the experimentally determined temperature dependence of the exciton energy gap. By fitting the equation to the experimental data we obtain the unrenormalized exciton binding energy $E_0 = 3.214$ eV and this result is in excellent agreement with the work of Göbel et al. [3]. Further to this we obtain the value of $A_{Cu} \approx 0.00301$ eV^2 amu and $A_{Cl} \approx -0.04917$ eV^2 amu. These are also very close to the values previously reported for sputtered [6] and evaporated CuCl films [5]. In addition the Z_3 exciton binding energy blue shift for the CuCl nanocrystalline hybrid films of about 41 meV for a temperature increase from 15 K to room temperature is also in good agreement with Ref. [3]. This blue shift for the CuCl nanocrystalline hybrid films can be understood in terms of a local empirical pseudopotential approach for the copper ion vibrations [56], which includes a shifting of remote d-like (copper) plane waves to a lower energy, so that they are close to the chlorine atomic p levels, and allows for p-d mixing. According to Ref. [3], the resulting level splitting in the valence band is to a large extent determined by a Cu atomic pseudopotential. The introduction of a Debye–Waller factor to "weaken" this pseudopotential with increasing temperature results in a decreasing hybridization energy. This lowers the top of the valence band and therefore the band gap increases with increasing temperature.

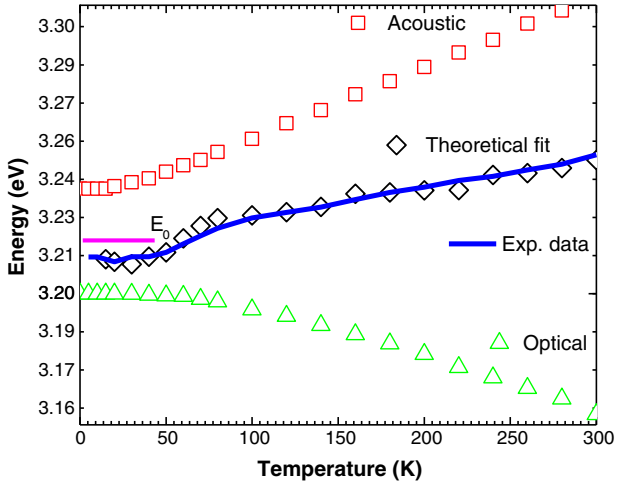

Fig. 7. Z_3 free exciton emission peak position shift as a function of with temperature; the solid line is the theoretical fit.

4. Conclusions

We have investigated the systematic temperature dependence of the photoluminescence of CuCl nanocrystalline hybrid films deposited via spin coating across a temperature range of 15 K to room temperature. The power dependent PL measurement confirmed the existence of both free biexciton (M) and bound biexciton (N_1) emission. At low temperatures we confirm that acoustic phonons are responsible for PL line width broadening and above 120 K the LO optical phonons are responsible the Z_3 excitonic FWHM broadening. The Z_3 exciton energy gap exhibits a blue shift of 3 meV at 15 K, which may be due to a dead layer effect near the CuCl nanocrystal surface. By increasing the temperature from 15 K to room temperature, the phonon induced interactions with exciton transitions have the following effects on the material properties: (a) PL intensity decrease (b) disappearance of transitions related to the impurity bound, free biexciton and impurity bound biexciton states due to the low binding energy of the impurity bound excitons, (c) PL emission line broadening due to an increase of the exciton–phonon interaction and (d) a blue shift of the energy gap due to the interaction of lattice vibrations with excitons. The PL properties of the nanocrystalline γ-CuCl hybrid films are comparable with vacuum deposited and sputtered CuCl films.

Acknowledgement

This project was funded by the Science Foundation Ireland Research Frontiers Programme (Project #06/RFP/ENE/027), Enterprise Ireland Commercialisation Fund for Technology Development (Project #CFTD/07/IT/331) and part-funded by the Irish Higher Education Authority PRTLI "INSPIRE" project.

References

[1] L. ÓReilly, A. Mitra, G. Natarajan, O.F. Lucas, P.J. McNally, S. Daniels, D.C. Cameron, A. Reader, A.L. Bradley, Impact on structural, optical and electrical properties of CuCl by incorporation of Zn for n-type doping, J. Cryst. Growth 287 (2006) 139.

[2] M.M. Alam, F. Olabanji Lucas, D. Danieluk, A.L. Bradley, K.V. Rajani, S. Daniels, P.J. McNally, Hybrid organic-inorganic spin-on-glass CuCl films for optoelectronic applications, J. Phys. D. Appl. Phys. 42 (2009) 225307.

[3] A. Göbel, T. Ruf, M. Cardona, C.T. Lin, J. Wrzesinski, M. Steube, K. Reimann, J.C. Merle, M. Joucla, Effects of the isotopic composition on the fundamental gap of CuCl, Phys. Rev. B 57 (1998) 15183.

[4] D. Danieluk, A. Bradley, A. Mitra, L. O'Reilly, O.F. Lucas, A. Cowley, P.J. McNally, B. Foy, E. McGlynn, Optical properties of undoped and oxygen doped CuCl films on silicon substrates, J. Mater. Sci. Mater. Electron. 20 (2009) S76.

[5] A. Mitra, L. O'Reilly, O.F. Lucas, G. Natarajan, D. Danieluk, A.L. Bradley, P.J. McNally, S. Daniels, D.C. Cameron, A. Reader, M. Martinez-Rosas, Optical properties of CuCl films on silicon substrates, J. Phys. Stat. Sol. 245 (2008) 2808.

[6] G. Natarajan, A. Mitra, S. Daniels, D.C. Cameron, P.J. McNally, Temperature dependent optical properties of UV emitting γ-CuCl thin films, Thin Solid Films 516 (2008) 1439.

[7] S. Park, I. Kim, K. Jang, S. Kim, C.D. Kim, Y. Yee, G. Jeen, Photo-luminescence properties of CuCl quantum dots and the dependence of biexciton formation rates on quantum dot sizes, J. Phys. Soc. Jpn. 70 (2001) 3723.

[8] Y. Masumoto, T. Kawamura, K. Era, Biexciton lasing in CuCl quantum dots, Appl. Phys. Lett. 62 (1993) 225.

[9] H. Shibata, Negative thermal quenching curves in photoluminescence of solids, Jpn. J. Appl. Phys. 37 (1998) 550.

[10] J.I. Pankove, Optical Properties in Semiconductor, Dover Publications, New York, 1971. 160.

[11] E.W. Williams, H.B. Bebb, Semiconductor and Semimetal, 8Academic Press, New York and London, 1972. 32.

[12] E.H. Bogardus, H.B. Bebb, Bound-exciton, free-exciton, band-acceptor, donor-acceptor, and auger recombination in GaAs, Phys. Rev. 176 (1968) 993.

[13] D. Bimberg, M. Sondergeld, E. Grobe, Thermal dissociation of excitons bounds to neutral acceptors in high-purity GaAs, Phys. Rev. B 4 (1971) 3451.
[14] F.E. Williams, H. Eyring, The mechanism of the luminescence of solids, J. Chem. Phys. 15 (1947) 289.
[15] S.R. Forrest, Ultrathin organic films grown by organic molecular beam deposition and related techniques, Chem. Rev. 97 (1997) 1793.
[16] L. Torsi, A. Dodabalapur, L. Rothberg, A. Fung, H.E. Katz, Intrinsic transport properties and performance limits of organic field-effect transistors, Science 272 (1996) 1462.
[17] F. Gamier, R. Hajlaoui, A. Yassar, P. Srivastava, All-polymer field-effect transistor realized by printing techniques, Science 265 (1994) 1684.
[18] M. Ueta, H. Kanzaki, K. Kobayashi, Y. Toyozawa, E. Hanumara, Excitonic Processes in Solids, 122Springer, Berlin, 1986.
[19] N. Nagasawa, N. Nakata, Y. Doi, M. Ueta, Generation of excitonic molecules by giant two-photon absorption in CuCl and their Bose condensation, J. Phys. Soc. Jpn. 39 (1975) 987.
[20] J.I. Pankove, Optical Processes in Semiconductors, 123Prentice-Hall, Englewood Cliffs NJ, 1971.
[21] S. Yano, T. Goto, T. Itoh, A. Kasuya, Dynamics of excitons and biexcitons in CuCl nanocrystals embedded in NaCl at 2 K, Phys. Rev. B 55 (1997) 1667.
[22] A. Musiał, G. Sęk, P. Podemski, M. Syperek, J. Misiewicz, A. Löffler, S. Höfling, A. Forchel, Excitonic complexes in InGaAs/GaAs quantum dash structures, J. Phys. Conf. Ser. 245 (2010) 012054.
[23] R.T. Phillips, D.J. Lovering, G.J. Denton, G.W. Smith, Biexciton creation and recombination in a GaAs quantum well, Phys. Rev. B 45 (1992) 4308.
[24] Y. Masumoto, S. Okamoto, S. Katayangi, Biexciton binding energy in CuCl quantum dots, Phys. Rev. B 50 (1994) 18658.
[25] K. Kouyama, M. Inoue, Y. Inose, N. Suzuki, H. Sekiguchi, H. Kunugita, K. Ema, A. Kikuchi, K. Kishino, Photoluminescence of exciton and biexciton in GaN nanocolumns, J. Lumin. 128 (2008) 969.
[26] A. Yamamoto, K. Miyajima, T. Goto, H.J. Ko, T. Yao, Bound biexciton photoluminescence in ZnO epitaxial thin films, (pages 871–875) Phys. Stat. Sol. B 229 (2002) 871.
[27] K. Edamatsu, G. Oohata, R. Shimizu, T. Itoh, Generation of ultraviolet entangled photons in a semiconductor, Nature (London) 431 (2004) 167.
[28] H.J. Lozykowski, V.K. Shastri, Excitonic and Raman properties of ZnSe/Zn1-×Cd×Se strained-layer quantum wells, J. Appl. Phys. 69 (1991) 3235.
[29] W. Bala, Z. Ukasiak, M.R. Barz, P. Dalasiski, A. Bratkowski, D. Bauman, R. Hertmanowski, Photoluminescence characterization of vacuum deposited PTCDA thin films, Opto-Electron. Rev. 12 (2004) 445.
[30] K. Saito, M. Hasuo, T. Hatano, N. Nagasawa, Band gap energy and binding energies of Z3-excitions in CuCl, Solid State Commun. 94 (1995) 33.
[31] T. Goto, T. Takahashni, M. Ueta, Exciton luminescence of CuCl, CuBr and CuI single crystals, J. Phys. Soc. Jpn. 24 (1968) 314.
[32] Xiangxin Liu, Photoluminescence and Extended X-ray Absorption Fine Structure Studies on CdTe Material, (PhD thesis) University of Toledo, Toledo, OH, 2006. 80.
[33] M. Cardona, Optical properties of the silver and cuprous halides, Phys. Rev. 129 (1963) 69.
[34] M. Nakayama, H. Ichida, H. Nishimura, Bound-biexciton photoluminescence in CuCl thin films grown by vacuum deposition, J. Phys. Condens. Matter 11 (1999) 7653.
[35] D. Kovalev, B. Averboukh, D. Volm, B.K. Meyer, H. Amano, I. Akasaki, Free exciton emission in GaN, Phys. Rev. B 54 (1996) 2518.
[36] A.K. Viswanath, I. Lee, S. Yu, D. Kim, Y. Choi, C. Hong, Photoluminescence studies of excitonic transitions in GaN epitaxial layers, J. Appl. Phys. 84 (1998) 3848.
[37] D.K. Shuh, R.S. Williams, Line-shape and lifetime studies of exciton luminescence from confined CuCl thin films, Phys. Rev. B 44 (1991) 5827.
[38] B. Damilano, N. Grandjean, S. Dalmasso, J. Massies, Room-temperature blue-green emission from InGaN/GaN quantum dots made by strain-induced islanding growth, Appl. Phys. Lett. 75 (1999) 3751.
[39] X. Liu, X. Wu, H. Cao, R.P.H. Chang, Growth mechanism and properties of ZnO nanorods synthesized by plasma-enhanced chemical vapor deposition, J. Appl. Phys. 95 (2004) 3141.
[40] Y. Kaifu, T. Komatsu, Exciton line-width and exciton-phonon interaction in CuCl, Phys. Status Solidi B 48 (1971) K125.
[41] T. Wamura, Y. Masumoto, T. Kawamura, Size-dependent homogeneous linewidth of Z_3 exciton absorption spectra in CuCl microcrystals, J. Appl. Phys. Lett. 59 (1991) 1758.
[42] A.S. Castillo, F.P. Rodrıguez, Quantization of longitudinal excitons in CuCl thin films, J. Appl. Phys. 90 (2001) 3662.
[43] K. Reimann, S.T. Rubenacke, Two-photon absorption in CuCl and CuBr under hydrostatic pressure, Phys. Rev. B 49 (1994) 11021.
[44] A. Blacha, S. Ves, M. Cardona, Effects of uniaxial strain on the exciton spectra of CuCl, CuBr, and CuI, Phys. Rev. B 27 (1983) 6346.
[45] K. Reimann, M. Haselhoff, S.T. Rubenacke, M. Steube, Determination of the pressure dependence of band-structure parameters by two-photon spectroscopy, Phys. Status Solidi B 198 (1996) 71.
[46] L.E. Brus, Electron-electron and electron-hole interactions in small semiconductor crystallites: The size dependence of the lowest excited electronic state, J. Chem. Phys. 80 (1984) 4403.
[47] S. Nikitine, Theory of stark effect of excitons in report of the international conference on the physics of semiconductors, Progr. Semicond. 6 (1962) 235.
[48] T. Koda, T. Murahashi, T. Mitani, S. Sakoda, Y. Onodera, Effects of uniaxial stress on excitons in CuCl, Phys. Rev. B 5 (1972) 705.
[49] H.C. Ong, A.X.E. Zhu, G.T. Du, Dependence of the excitonic transition energies and mosaicity on residual strain in ZnO thin films, Appl. Phys. Lett. 80 (2002) 941.
[50] International Centre for Diffraction, JCPDS Card No. 06-344, 1997.
[51] D. Kim, M. Nakayama, O. Kojima, H. Ichida, T. Nakanishi, H. Nishimura, Thermal-strain-induced splitting of heavy- and light-hole exciton energies in CuI thin films grown by vacuum evaporation, Phys. Rev. B 60 (1999) 13879.
[52] Y. Kayanuma, Quantum-size effects of interacting electrons and holes in semiconductor microcrystals with spherical shape, Phys. Rev. B 38 (1988) 9797.
[53] C.I. Yu, T. Goto, M. Ueta, Emission of cuprous halide crystals at high density excitation, J. Phys. Soc. Jpn. 34 (1973) 693.
[54] Y.P. Varshini, Temperature dependence of the energy gap in semiconductors, Phys. E. 34 (1967) 149.
[55] X.T. Zhang, Y.C. Liu, Z.Z. Zhi, J.Y. Zhang, Y.M. Lu, D.Z. Shen, W. Xu, X.W. Fan, X.G. Kong, Temperature dependence of excitonic luminescence from nanocrystalline ZnO films, J. Lumin. 99 (2002) 149.
[56] N. Garro, A. Cantarero, M. Cardona, T. Ruf, A. Göbel, C. Lin, K. Reimann, S. Rtibenacke, M. Steube, Electron-phonon interaction at the direct gap of the copper halides, Solid State Commun. 98 (1996) 27.